



### Air-sea interactions

A. LOFFE<sup>1</sup> and A. BAH

Mécanique des Fluides géophysiques, Université de Liège, Belgium

G. SCHAYES

Institut d'Astronomie et de Géophysique, Université Catholique de Louvain, Louvain-la-Neuve, Belgium

## Air-sea interactions

A. LOFFET<sup>1</sup> and A. BAH

Mécanique des Fluides géophysiques, Université de Liège, Belgium

G. SCHAYES

Institut d'Astronomie et de Géophysique, Université Catholique de Louvain, Louvain-la-Neuve, Belgium

### Introduction

Of late years, the investigation of air-sea interactions and the study of their effect on the dynamics of the ocean and the atmosphere have gained considerable importance.

Much work is at the moment being devoted to the measurement and parameterization of the different transfers occurring at the air-water interface. These consist mainly of fluxes of mass (water vapour, gases, pollutants), heat (short and long wave radiation, latent and sensible heat), momentum and mechanical energy.

At the local scale, these fluxes act as boundary conditions on the oceanic and atmospheric systems. They supply almost all the energy for circulations and turbulence in the ocean. They determine the state of the sea and of the water immediately below the interface. (A very important part of all the solar radiation absorbed below the bottom of the atmosphere is stored temporarily in the upper layers of the ocean). This portion of the sea being most under their influence is also the place where a very important biological activity occurs, which constitutes a crucial link in the food chain in the sea. Besides, they determine the state of the atmospheric lower layers, their stability, and their temperature, moisture and velocity distributions.

---

1. Aspirant F.N.R.S.

Moreover, these fluxes are also of primary importance at the large scale : the climate of the earth is a very intricate system involving land, sea and air. As constant transfers occur continuously between the different components, the dynamics of the climate must take the oceanic and atmospheric dynamics into account, with all their interactions.

In this paper, we will present some of the work we are at present undertaking in this field.

In a first paragraph, the radiative and turbulent energy fluxes will be detailed ; several methods of measurement we are using will be described and compared, and the first experimental results will be presented.

In a second paragraph, some features of the atmospheric boundary layer and the ocean mixed layer and thermocline will be depicted. The general equations governing both phenomena will be introduced and different modelling approaches we are using will be described.

A last paragraph will introduce a large scale air-sea interaction problem and present some preliminary results: the ocean dynamics of the Gulf of Guinea (laying stress on the upwelling problem), and its possible connection with the climate of the Sahel area.

## 1.- Energy transfers and their measurement

### 1.1.- THE BASIC ENERGY TRANSFERS

A general view of the various energy fluxes involved in air-sea interactions is shown in figure 1. The two broad classes of exchanges are clearly depicted : radiative and turbulent.

#### 1.1.1.- Radiative transfers

The basic source of energy is the sun. Its light undergoes many transformations before reaching the sea level. Diffusion and absorption by atmospheric molecules and clouds may reduce in a considerable way the energy arriving at the surface. Some light is also reflected by the sea surface (albedo), so that the remaining energy really absorbed in the upper layers of the ocean may vary within wide limits according to the season, time of the day and cloudiness.

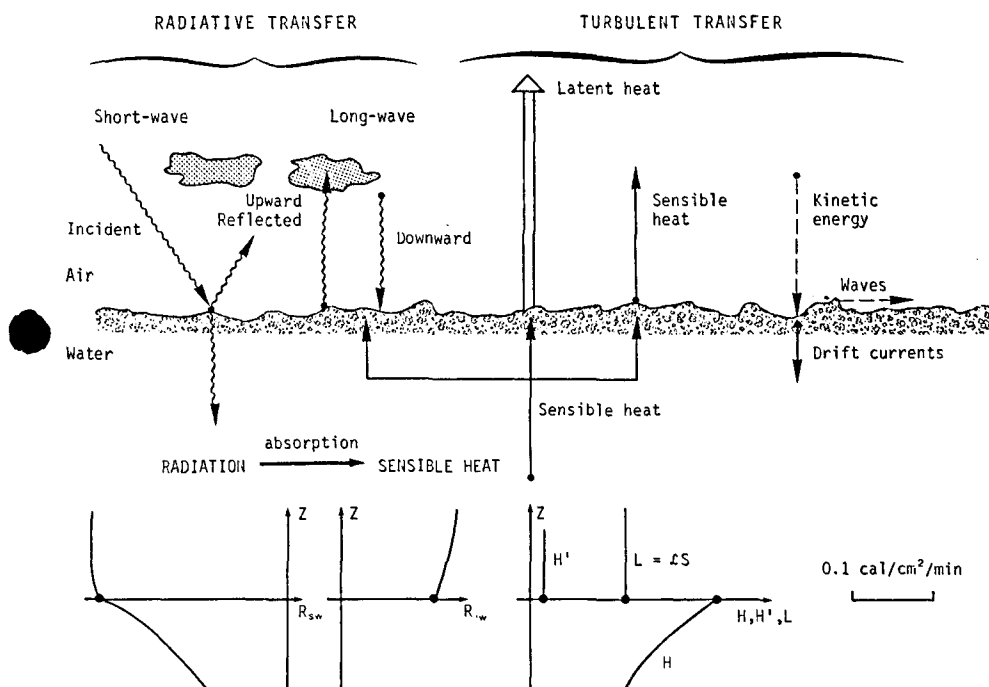


fig. 1.

Schematic display of energy transfers and transformations in the vicinity of the ocean-atmosphere interface, and the corresponding upward fluxes, assuming a steady-state situation.

In the infra-red part of the spectrum, a more complex equilibrium is reached between thermal emission from the sea surface and from the atmosphere above it. This is due to the high absorptive power of water vapour, of course present in large quantities in the marine atmosphere.

#### 1.1.2.- Turbulent transfers

Friction on the sea surface generates turbulence in the air, enabling a turbulent transfer of energy. Some quantity of heat is exchanged in this way between the sea surface and the air, but the biggest part of the energy is extracted from the sea surface by evaporation of water, thus by transfer of latent heat.

Some part of the mechanical energy of the air is also transferred to the ocean (waves, current, oceanic turbulence).

The oceanic medium, subject to all these atmospheric inputs responds in its own way. The characteristics of its surface are modified (temperature, roughness), and this can in its turn affect the lower atmosphere. This is the basic feed-back mechanism of air-sea interactions.

This brief survey of the main exchanges between the atmosphere and the ocean makes the complexity of the problem in its generality obvious. This is the reason why most of the modelling approaches have to divide the task into smaller ones.

### 1.1.3.- Energy balance at the sea level

If  $S_0$  denotes the solar incoming radiation flux and  $\alpha$  the albedo of the sea surface, the following relation states that the sum of all energy fluxes is equal to zero :

$$I_0 - I_L' + I_L'' - H - E + W = 0 \quad (1)$$

(a positive sign means a gain of energy for the surface)

where

$$I_0 = S_0 (1 - \alpha) ,$$

$I_L'$  is the infra-red emission of the surface,  $I_L''$  is the infra-red emission from the atmosphere,  $H$  is the sensible heat flux (to the atmosphere),  $E$  is the latent heat flux (to the atmosphere),  $W$  is the sensible heat flux in the sea (positive upwards).

## 1.2.- THE ESTIMATION OF THE FLUXES

### 1.2.1.- Radiative transfers

Measurements of radiative fluxes are difficult at sea mainly because of sea spray. After a few days in normal conditions, the sensors are covered with a film of salt, and a close watch on the instruments must be kept to ensure enough accuracy in the measurements. For that reason, only solar radiative flux can be obtained in coastal stations without much trouble. The albedo of the sea surface can now be fairly well determined

from tables of sea surface reflectivity as a function of sun height, cloud cover and sea state (Krauss, 1972). Because of the sea spray, radiative measurements at sea can only be performed during special campaigns when a constant survey of the equipment is possible. The global or net radiative fluxes (upwards-downwards, both visible and infra-red) can then be measured. The only problem is to keep the sensor horizontal and to take into account the solid angle under which the sensor "sees" the boat.

### 1.2.2.- Turbulent transfers

There is no simple and direct way of measuring the turbulent energy fluxes, and indirect methods must be used. We shall briefly describe here four methods used to determine the fluxes at the local scale. They are :

- a) drag coefficient formulas
- b) similarity and surface layer theory
- c) direct measurement of fluctuation covariances
- d) spectral methods

#### a) *Drag coefficient*

This is the simplest way of estimating the fluxes. The only quantities needed are the wind speed at some standard level (usually 10 m) above the sea surface, the air temperature and humidity at the same level, and the sea surface temperature.

In the turbulence theory, the fluxes are given by :

$$\tau = \rho_a u_*^2 \quad (2)$$

$$H = - \rho_a C_{pa} u_* T_* \quad (3)$$

$$E = - \rho_a L u_* q_* \quad (4)$$

where  $\tau$  is the surface stress or flux of momentum,  $H$  and  $E$  are the sensible and latent heat fluxes,  $\rho_a$  is the density of the air,  $C_{pa}$  is the heat capacity of the air at constant pressure,  $L$  is the latent heat of vaporization of the water,  $u_*$  is the friction velocity in the air,  $T_*$  and  $q_*$  are the temperature and humidity scales of turbulent fluctuations.

The first drag coefficient  $C_D$  is defined as the square of the ratio of the friction velocity  $u_*$  to the wind speed  $V$  measured at the standard level, i.e. :

$$u_* = C_D^{\frac{1}{2}} V_{10} .$$

The other coefficients  $C_E$  and  $C_H$  can be introduced in a similar way. The drag formulas are thus :

$$\tau = \rho_a C_D V_{10}^2 \quad (5)$$

$$H = - \rho_a C_{Pa} C_H V_{10} (T_{10} - T_w) \quad (6)$$

$$E = - \rho_a L C_E V_{10} (q_{10} - q_w) \quad (7)$$

where  $T_{10}$  is the air temperature at 10 m height,  $q_{10}$  is the air humidity at 10 m height,  $T_w$  is the water temperature,  $q_w$  is the specific humidity of saturated air at the water temperature (this quantity is determined from  $T_w$  and the tables of thermodynamic properties of water vapour).

In fact, the drag coefficients  $C_D$ ,  $C_E$  and  $C_H$  simply relate the measurable quantities to unmeasurable ones. These coefficients have been carefully determined in special measurement campaigns by a best fit to the observed flux data. Unfortunately, there is a wide variety of  $C_D$  in the literature. We present here one of the latest version reported by Friehe and Gibson (1978). If

$$\Delta T = T_w - T_{10} ,$$

$$C_D = 10^{-3} \times (0.63 + 0.066 V_{10}) \quad (8)$$

$$C_H = \begin{cases} 10^{-3} \times (2 + 0.97 V_{10} \Delta T) \\ 10^{-3} \times (1.46 V_{10} \Delta T) \end{cases} \quad \text{if} \quad V_{10} \Delta T \begin{cases} < 25 \text{ m s}^{-1} \text{ K} \\ > 25 \text{ m s}^{-1} \text{ K} \end{cases} \quad (9)$$

$$C = 10^{-3} \times 1.32 \quad (10)$$

( $V_{10}$  in  $\text{m s}^{-1}$ ,  $T$  in Kelvins).

As a rule, the  $C_D$ 's are increasing with increasing wind speed, because of the increasing roughness length  $z_0$  of the sea.

This is the simplest way of obtaining valuable estimates of the fluxes. However, a non negligible scatter of  $C_D$  values among different authors may question the general applicability of the method.

b) *Similarity theory — Surface layer formulas*

The original similarity theory of Monin and Obukov published in 1954 has been widely used recently since the determination of the functions by Businger (1973). The theory stipulates that the vertical non dimensionalised wind, temperature and humidity gradients are only function of a non dimensional height  $\xi = z/L$ , where  $L$  is the Monin-Obukov length scale, defined as :

$$L = \frac{\bar{T} u_*^2}{kgT_*} \quad (11)$$

$g$  is the acceleration of gravity and  $\bar{T}$  the mean temperature,  $k$  is the Von Karman constant ( $k = 0.35$ ).

Thus

$$\left\{ \begin{array}{l} \frac{kz}{u_*} \frac{\partial \bar{u}}{\partial z} = \phi_M(\xi) \\ \frac{kz}{T_*} \frac{\partial \bar{T}}{\partial z} = \phi_H(\xi) \\ \frac{kz}{q_*} \frac{\partial \bar{q}}{\partial z} = \phi_E(\xi) \end{array} \right. \quad (12)$$

The  $\phi_i$  ( $i = M, H, E$ ) have now a well known analytical form (Businger, 1973).

The relations (I.12) can be integrated from 0 (or  $z_0$ ) to the standard level of measurement (usually 10 m), yielding the integrated form  $\psi_i$  of the  $\phi_i$ . We have then :



$$\left\{ \begin{array}{l} u_* = \frac{k V_{10}}{\ln \frac{z}{z_0} - \psi_M} \\ T_* = \frac{k (T_{10} - T_w)}{0.74 \ln \frac{z}{z_0} - \psi_H} \\ q_* = \frac{k (q_{10} - q_w)}{0.74 \ln \frac{z}{z_0} - \psi_E} \end{array} \right. \quad (13)$$

We obtain in this way an implicit set of equations that can be solved iteratively to have  $L$ ,  $u_*$ ,  $T_*$  and  $q_*$  from the observed  $V_{10}$ ,  $T_{10}$ ,  $T_w$  and  $q_w$ . The fluxes can then be obtained directly from equations (2) to (4). It is important to note that in order to use equations (13), an adequate value of  $z_0$  must be determined independently, generally as a function of  $V_{10}$ .

c) *Direct method*

With fast response sensors and a fixed, stable frame of reference, the fluctuating eddies in the air may be resolved and the turbulent fluxes can be directly expressed as the covariances of the fluctuations of the vertical wind component and the other quantity. Thus :

$$\left\{ \begin{array}{l} \tau = - \rho_a \overline{u'w'} \\ H = \rho_a C_{pa} \overline{T'w'} \\ E = \rho_a L \overline{q'w'} \end{array} \right. \quad (14)$$

(Here an overbar denotes a time average over an adequate period, generally of the order of a few tens of minutes, and primes denote fluctuations around the mean).

Comparing (I.2 to I.5) with (I.14) leads immediately to :

$$\begin{cases} \overline{u'w'} = -u_*^2 \\ \overline{T'w'} = -u_*T_* \\ \overline{q'w'} = -u_*q_* \end{cases} \quad (15)$$

which can be used to define the velocity, temperature and humidity scales  $u_*$ ,  $T_*$  and  $q_*$ .

This technique may be considered as an absolute measurement of the fluxes (a reference one), but it needs sensors able to respond to frequencies up to a few Hz in order to pick up the portion of the flux due to small eddies. In the atmosphere, this implies a sampling frequency of the order of 10 Hz.

The other important point is that the verticality of the sensor must be accurately set, and must remain unchanged. Equations (I.14) show that  $w'$  is the leading factor. Even a very small deviation of the sensor from the vertical should induce the effect of  $u$  or  $v$  in the measured  $w$  (since generally  $\bar{u} \approx \bar{v} \gg \bar{w}$ ). This implies the use of a fixed rigid support for the instrument (a pile e.g.) and excludes any simple system (as usual buoys or boats).

#### d) *Spectral method*

This promising method will be briefly outlined here. For details, one can refer to Champagne et al. (1977).

In the inertial subrange of turbulence, the spectrum of wind fluctuations follows the Kolmogorov's law :

$$S_u(n) = \alpha_1 u_*^{\frac{2}{3}} \epsilon^{\frac{2}{3}} n^{-\frac{5}{3}} \quad (16)$$

where  $\alpha_1$  is a constant  $\approx 0.55$ ,  $\epsilon$  is the dissipation rate,  $n$  is the frequency measured at a fixed point in space.

In neutral conditions, the wind profile follows the logarithmic law :

$$\frac{\partial u}{\partial z} = \frac{u_*}{kz} .$$

As the turbulent energy balance in the stationary case is

$$- \overline{u'w'} \frac{\partial u}{\partial z} = \epsilon ,$$

we have

$$u_* = (k \epsilon z)^{\frac{1}{3}} .$$

In the non-neutral case, it can be shown that this relation becomes :

$$u_* = \left[ \frac{k \epsilon z}{\left[ 1 + 0.5 \left| \frac{z}{L} \right|^{2/3} \right]^{3/2}} \right]^{1/3} \quad (17)$$

As  $\epsilon$  can be found from (16), equation (2) gives an evaluation of the momentum flux if  $L$  is known.

A similar procedure can be followed for temperature and humidity : the spectrum of temperature fluctuations follows the law

$$S_\theta(n) = \beta_\theta \chi_\theta u^{\frac{2}{3}} \epsilon^{-\frac{1}{3}} n^{-\frac{5}{3}} \quad (18)$$

where  $\beta_\theta$  is a constant  $\approx 0.4$ ,  $\chi_\theta$  is the dissipation rate for temperature fluctuations (to be determined). The use of a similar hypothesis for the temperature profile leads to the following expression for the temperature scale :

$$T_* = - \left[ \frac{k z \chi_\theta}{2 u_* \phi_H} \right]^{\frac{1}{2}}$$

where  $\phi_H$  is the similarity function for heat.

The heat flux is then found by equation (3).

A quite similar relation is also established for  $q_*$ , but at the present time, no experimental confirmation exists for it.

#### e) Comparison of the methods

Table 1 summarizes the needs and advantages of each method.

The last two methods require instruments capable of measuring frequencies over 1 Hz in the fluctuations. The ideal instrument for this purpose is the sonic anemometer. The Gill anemometer we have can also be used, if it is not too close to the sea surface.

Table 1

Comparison of the methods used to determine the turbulent fluxes

Method	Data needed	Instrument needed	Comments	Maximum expected error
A.Drag coefficient	$T_{10}$ , $T_w$ , $V_{10}$ , $q_{10}$ + choice of drag coefficients formulas	Simple instruments measuring mean values	Very fast method	$\pm 40 \%$
B.Similarity Monin-Obukov	$T_{10}$ , $T_w$ , $V_{10}$ , $q_{10}$ + estimated $z_0$	Use of buoy possible.	Iterative method	$\pm 40 \%$
C.Direct covariance	$u$ , $v$ , $w$ , $T$ , $q$	Fast response instruments to measure fluctuating quantities. Fixed frame of reference (tower or mast fixed on bottom) Vertical must be accurately defined.	Basic technique of flux determination Difficult method at sea.	$\pm 10 \%$
D.Spectral	$u$ , $T$ , $q$	Fast response instruments to measure fluctuating quantities. Fixed frame of reference not necessary. Vertical wind speed not needed. Use of buoy should be possible.		$\pm 20 \%$ (?)

## 1.3.- A FEW RESULTS

A buoy has been operated in common by the Institut Royal Météorologique (I.R.M.), the University of Liège, and the University of Louvain-La-Neuve, during two summer campaigns at STARESO, the oceanographic station of the University of Liège in Calvi, Corsica.

The available data are summarized in table 2.

Table 2  
Data measured by the I.R.M. buoy in Calvi

Campaign	Period of recording	Measured parameters
Summer 1977	14-7-77 to 10-8-77 (with interruptions)	Wind speed Air temperature } at 6 m height Sea surface temperature at - 2 m
Summer 1978	9-7-78 to 9-8-78	Wind speed Wind direction } at 6 m height Air temperature Wind speed Air temperature } at 2 m height Water temperature at - 2 m

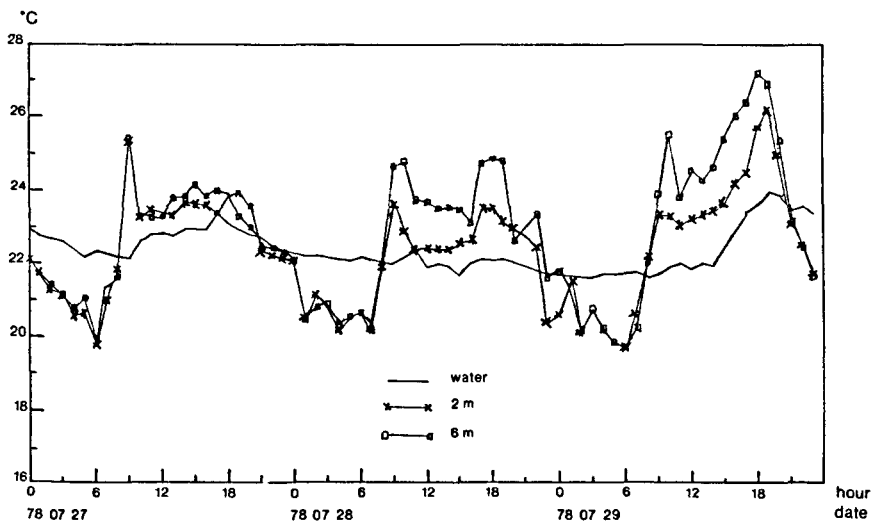


fig. 2.

Sample of observed temperatures in the Bay of Calvi with the I.R.M. buoy

Figures 2 and 3 show a sample of the measured data. Figure 4 shows the estimated fluxes for the 1978 summer campaign.

The reader may refer to the work of Clement (1979) for complete fluxes calculations and comparisons. The complete set of data is available at the I.R.M.

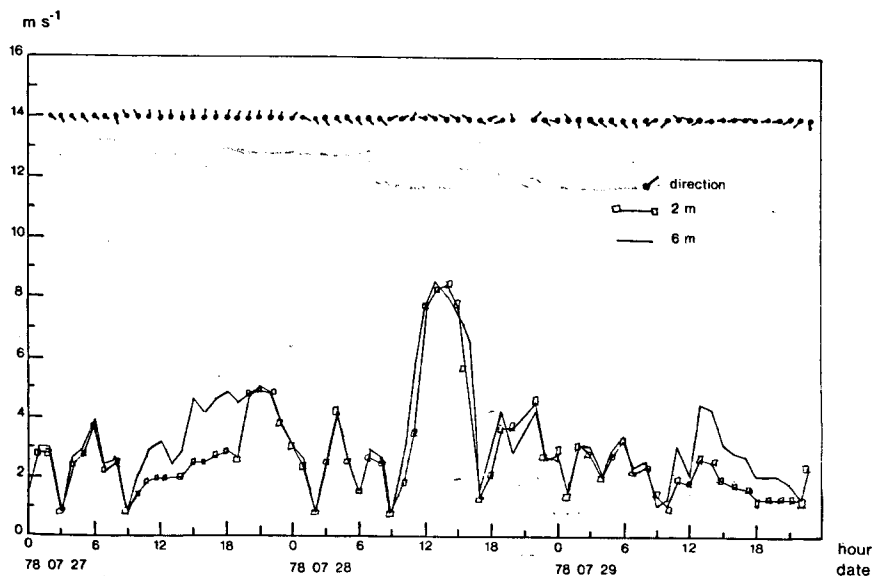


fig. 3.

Sample of observed wind speed and direction in the Bay of Calvi with the I.R.M. buoy

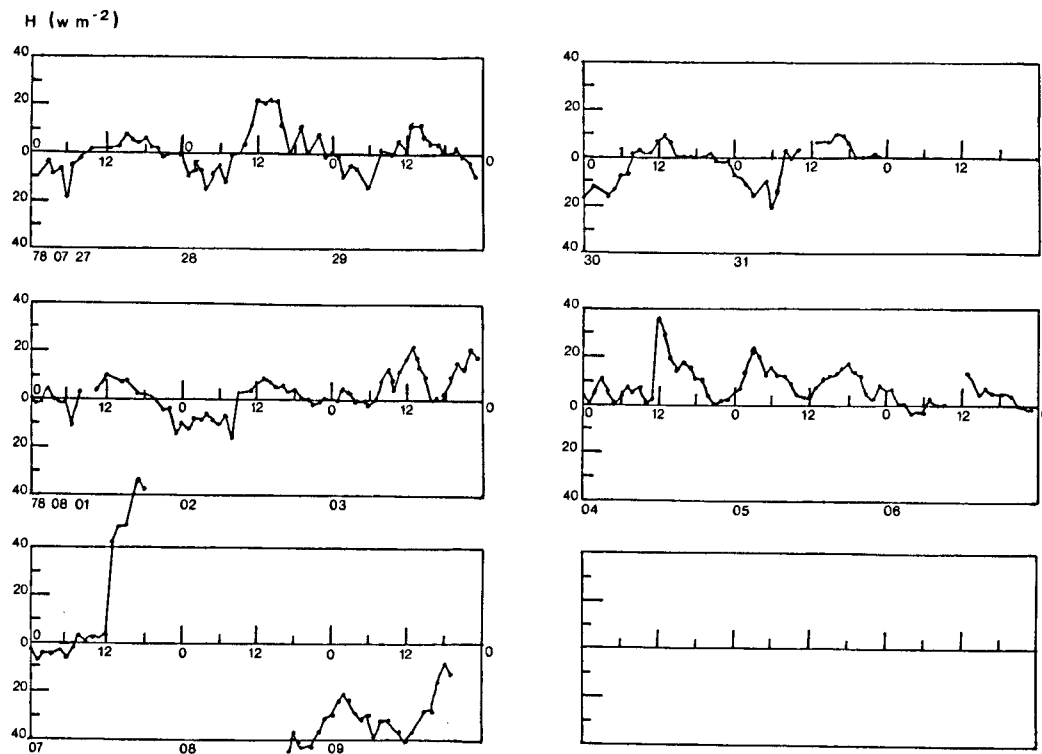


fig. 4.

Estimated heat fluxes from 27-07 to 09-08-1978

## 2.- The boundary layers in the atmosphere and the ocean

In the preceding section, several processes occurring close to the sea surface (at a few meters height) have been described in order to measure the turbulent fluxes at the interface.

As mentioned in the introduction, the fluxes act also as lower boundary conditions for the atmospheric boundary layer, i.e. the layer in which turbulent exchanges of momentum, heat and moisture take place. Typically, this layer is from 500 to 1500 meters high. Above this level, the friction of the sea surface is no more felt, and the air flux is normally non turbulent.

They act also as boundary inputs for the upper layers of the ocean. However, the ocean has a much larger thermic and dynamic inertia than the atmosphere, and very often exhibits an important stratification which acts as a barrier for the exchanges with lower water layers. This stratification is mainly due to heat and salinity.

Before starting with the equations used to model the atmospheric boundary layer and the upper layers of the ocean, it is interesting to have a look at the general characteristics of the ocean vertical thermal structure.

### 2.1.- MAIN FEATURES OF THE VERTICAL THERMAL STRUCTURE OF THE OCEAN

In this section, we shall not consider the recently discovered phenomenon of fine-scale stratification or microstructure in the ocean, although this could lead to a reconsideration of the modelling problem, but emphasize the coarser general structure of the oceanic waters. (Further informations about microstructure can be found in Fedorov, 1978).

In low and mid latitude areas, the mean vertical structure of the waters (disregarding annual or higher frequencies fluctuations) can be schematized by the existence of three different layers :

a) a surface layer, 50 to 200 m deep, where the temperature is close to its value at the surface ;

b) a layer in which the temperature decreases with depth and which extends itself below the first and down to 1000 m almost. This is the main or permanent thermocline.

c) deeper, the temperature gradient dies away : we are in the domain of the deep waters.



There are also some differences between the equatorial and mid-latitude areas : in the former ones, the waters are highly stratified and a well defined thermocline can be found ; in the latter ones, there is also a thermocline, but not so important and often deeper.

However, polar areas, many lakes and some enclosed seas (as the Mediterranean Sea) do not exhibit a permanent thermocline. This mean global structure is mainly the result of the large scale energetic exchanges with the atmosphere and the general oceanic circulation.

The layers close to the sea surface (0 - 100 m) undergo the influence of the exchanges with the atmosphere, and these have several well or less marked periodicities (seasonal, diurnal, synoptic,...). Heat fluxes depend locally on the season, hour of the day and atmospheric conditions. Mechanical energy transfers, depending mainly on the wind, can also exhibit a periodicity of a few days (synoptic, i.e. related to the development of atmospheric perturbation in our latitudes, e.g.). The advection can also take an important part locally.

In connection with the seasonal variations of the fluxes in mid and high latitude areas, a seasonal thermocline develops at the bottom of a layer often close to homogeneity in temperature. This thermocline appears in spring, develops in summer and dies away at the end of autumn. The temperature difference between the upper warm layers and the underlying fluid is more important at mid-latitude than in polar areas. In low latitude areas, the seasons are not so distinct, and there is almost no variation across the year.

Finally, diurnal or synoptic variations in the fluxes can also induce diurnal or transitory thermocline structures. In special circumstances, a succession of transitory thermoclines can be observed above the seasonal thermocline, related to the evolution of the fluxes in the preceding days.

It should again be noticed that polar areas, some lakes and enclosed seas as the Mediterranean Sea have only seasonal, diurnal and transitory thermoclines.

One important problem, and also one of the best documented, is the study of the effect of a gust of wind causing mixing in the upper layers and entrainment of the underlying fluid. The new mixed layer can enclose old thermoclines and even reach the seasonal thermocline and modify it.

Figure 5 shows an example of a well develop mixed layer due to a sudden rise in wind force. The profiles were taken at STARESO, Calvi, Corsica.

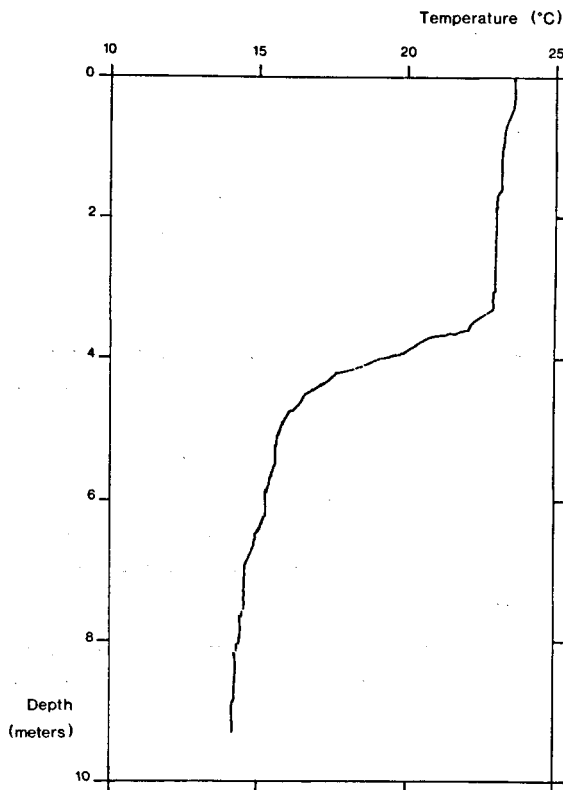


fig. 5.

Vertical structure of the water temperature off Calvi, Corsica,  
after the passage of a gust of wind (10 m/s) [18-07-77]

One of our present aims is to model the dynamics of the upper oceanic layers at the different time scales. If the question of the mixed layer deepening is well documented, its later evolution and restructuration still set unresolved experimental and theoretical problems.

## 2.2.- BOUNDARY LAYER MODELLING

The fundamental hypotheses used for the modelling of the atmospheric boundary layer and of the oceanic upper mixed layer and thermocline are the following :

1) The Boussinesq approximation.

In the ocean

$$\rho = \rho_0 [1 - \alpha(T - T_0) + \beta(S - S_0)] , \quad \rho_0 = \rho(S_0, T_0)$$

where  $T$  is the temperature and  $S$  the salinity. In the atmosphere, a similar formula is introduced, involving potential temperature and water-vapour content.

2) The parameters are decomposed into a mean value (denoted by an overbar) and turbulent fluctuations. The equations for the mean values of the parameters are considered, as well as the equation for turbulent kinetic energy.

Nowadays, second order closure models are being developed. These consider also the equations for all second order covariances and use closure hypotheses for these equations. However, they involve many computation problems and in a first time, we will restrict ourselves to the former, simpler but more direct approach.

3) Horizontal homogeneity is also assumed. This hypothesis is realistic in the marine atmospheric boundary layer, because of the absence of topography. In the ocean, it is also realistic if we consider areas far enough from coastal areas and bottom effects.

We get in this way :

$$\frac{\partial u}{\partial t} = f(v - v_g) - \frac{\partial}{\partial z} \overline{u'w'} \quad (19)$$

$$\frac{\partial v}{\partial t} = -f(u - u_g) - \frac{\partial}{\partial z} \overline{v'w'} \quad (20)$$

$$\frac{\partial T}{\partial t} = -\frac{\partial}{\partial z} \overline{w'T'} + \frac{R}{\rho_{0_w} c_{p_w}} \quad (\text{ocean})$$

or

$$\frac{\partial \theta}{\partial t} = -\frac{\partial}{\partial z} \overline{w'\theta'} + \frac{R}{\rho_{0_a} c_{p_a}} \quad (\text{atmosphere}) \quad (21)$$

$$\frac{\partial S}{\partial t} = - \frac{\partial}{\partial z} \overline{w' S'} \quad (\text{ocean})$$

or

(22)

$$\frac{\partial q}{\partial t} = - \frac{\partial}{\partial z} \overline{w' q'} \quad (\text{atmosphere})$$

$$\frac{\partial e}{\partial t} = - \overline{u' w'} \frac{\partial u}{\partial z} - \overline{v' w'} \frac{\partial v}{\partial z} + \overline{w' b'} - \frac{\partial}{\partial z} \left[ \frac{\overline{p' w'}}{\rho_0} + \frac{\overline{u'^2 + v'^2 + w'^2}}{2} w' \right] - \epsilon \quad (23)$$

The frame of reference is dextrorsum, with  $z$  positive upwards. The over-bars have been omitted for mean speeds ( $u, v$ ), temperature, or potential temperature in the atmosphere ( $T, \theta$ ), salinity ( $S$ ), humidity ( $q$ ) and turbulent kinetic energy ( $e$ ).  $f$  is the Coriolis parameter and ( $u_g, v_g$ ) the geostrophic wind or current.  $\rho_0$  and  $c_p$  are related to the air, or the sea water,  $R$  is the divergence of the radiation flux,  $b'$  denotes the fluctuations of buoyancy  $b$  defined as  $b = -\frac{\rho - \rho_0}{\rho_0} g$ . An equation for buoyancy can be written instead of (21) and (22).

The right-hand side terms of the last equation have the following physical meaning :

$-\overline{u' w'} \frac{\partial u}{\partial z} - \overline{v' w'} \frac{\partial v}{\partial z}$  is the turbulence production due to shear in the mean wind or current ,

$\overline{b' w'}$  is a source or a sink of turbulent kinetic energy due to the buoyancy forces ,

$\frac{\partial}{\partial z} \left[ \frac{\overline{p' w'}}{\rho_0} + \frac{\overline{u'^2 + v'^2 + w'^2}}{2} w' \right]$  is a transport term of turbulence,

$\epsilon$  is the turbulent kinetic energy dissipation ( $\epsilon > 0$ ).

Closure hypotheses have to be introduced now in order to solve the system. We also need initial and boundary conditions for the different variables.

We will examine the particular cases of the atmospheric and oceanic boundary layers.

### 2.2.1.- Atmospheric boundary layer

The turbulent diffusivities  $K_M$ ,  $K_\theta$  and  $K_q$  are introduced :

$$-\overline{u'w'} = K_M \frac{\partial u}{\partial z} \quad ; \quad -\overline{v'w'} = K_M \frac{\partial v}{\partial z} \quad (24)$$

$$-\overline{w'\theta'} = K_\theta \frac{\partial \theta}{\partial z} \quad (25)$$

$$-\overline{w'q'} = K_q \frac{\partial q}{\partial z} \quad (26)$$

In this case, if we neglect the divergence of the radiation flux, equations (19) to (22) become :

$$\frac{\partial u}{\partial t} = f(v - v_g) + \frac{\partial}{\partial z} (K_M \frac{\partial u}{\partial z}) \quad (27)$$

$$\frac{\partial v}{\partial t} = -f(u - u_g) + \frac{\partial}{\partial z} (K_M \frac{\partial v}{\partial z}) \quad (28)$$

$$\frac{\partial \theta}{\partial t} = \frac{\partial}{\partial z} (K_\theta \frac{\partial \theta}{\partial z}) \quad (29)$$

$$\frac{\partial q}{\partial t} = \frac{\partial}{\partial z} (K_q \frac{\partial q}{\partial z}) \quad (30)$$

These four equations can be solved numerically if initial profiles of  $u$ ,  $v$ ,  $\theta$  and  $q$  are given as well as the temperature and humidity time evolution at the sea level. The  $K$ 's are used as parameters. Many kinds of ABL models have been devised assuming various forms of  $K(z)$  profiles. The interested reader can find a review of  $K(z)$  specifications in Yu (1977), Coantic (1978) and Schayes (1979).

A not complicated and realistic  $K$  formulation is based on equation (II.5). The introduction of the diffusivities and several hypotheses lead to :

$$\frac{\partial e}{\partial t} = K_M \left( \underbrace{\left[ \frac{\partial u}{\partial z} \right]^2}_{(a)} + \underbrace{\left[ \frac{\partial v}{\partial z} \right]^2}_{(b)} - 1.35 \frac{q}{\theta} \frac{\partial \theta}{\partial z} \right) + \underbrace{1.2 \frac{\partial}{\partial z} [K_M \frac{\partial e}{\partial z}]}_{(c)} - \underbrace{\epsilon}_{(d)} \quad (31)$$

where we find again the expressions for turbulent kinetic energy production

by wind shear (a), production or removal due to buoyancy (b), diffusion (c) and dissipation (d).

The dissipation  $\epsilon$  is frequently expressed as

$$\epsilon = c e^{\frac{3}{2}} \ell \quad (c \text{ is a constant})$$

and  $K_M$  is defined by

$$K_M = c \ell e^{\frac{1}{2}}$$

The set of equations is then closed if we specify the mixing length  $\ell$ . Various formulations exist among which the one of Blackadar is frequently used :

$$\ell = \frac{kz}{1 + \frac{kz}{\lambda}} \quad \text{or} \quad \frac{1}{\ell} = \frac{1}{\lambda} + \frac{1}{kz}$$

where

$$\ell = 2.7 \cdot 10^{-4} \left| \frac{U_g}{f} \right| \quad (U_g \text{ is the geostrophic wind}).$$

Up to this point, the model fits mainly continental ABL simulation. On land, turbulent processes are dominating due to the normally large temperature oscillation of the night and day sequence. Large instabilities can develop during the day, triggering convection. On the other hand, over the sea, the daily temperature oscillation (at sea level) is very much smaller, and instability does not develop in daytime (unless advection of cold air over warm water occurs).

Therefore, radiative and evaporation phenomena are as important as turbulent ones over the marine ABL and we must take the radiative term into account in (29).

$$\frac{\partial \theta}{\partial t} = \frac{\partial}{\partial z} \left[ K_\theta \frac{\partial \theta}{\partial z} \right] + \frac{R}{\rho_{0a} c_{\rho a}} \quad (32)$$

$$R = - \frac{\partial}{\partial z} (F' - F^*) \quad (33)$$

$R$  is the heating rate due to the divergence of the radiation flux density.  $F^*$  is the total radiative flux upwards, and  $F^\dagger$  the total radiative flux downwards at the considered level.

The  $F$ 's are computed by integrating the absorptivity - emissivity of water vapour at all levels above or below the considered level. For example  $F^*$  is given by :

$$F^*(z_1) = \int_{z_1}^{\infty} \sigma T^4 \frac{d\varepsilon(z_1, z)}{dz} dz \quad (34)$$

where  $\sigma$  is the Stefan constant (black body) and  $\varepsilon$  is here the emissivity of water vapour between levels  $z_1$  and  $z$ . A similar equation is used for  $F^\dagger$ .

Such a radiative model should simulate the marine ABL in a reasonably good way as far as advective phenomena are not important.

Let us notice two points now :

- this model does not take any condensation of water vapour into account, i.e. the presence or formation of clouds above the BL (medium and high clouds) and in the BL (low clouds), which affect considerably the radiative balance of the system. These important problems have not yet found a good solution. They are often parameterized in a crude way in order to avoid very long computation time.

- if horizontal homogeneity cannot be assumed, one has to turn to a two-dimensional or even a full three-dimensional model. This is however needed to represent phenomena as sea breeze along a coast, or non uniform meteorological situations, which unfortunately are not rare.

Input data for the models consist of initial profiles of wind, temperature and humidity, and the evolution of the sea temperature. These data are obtainable from standard radiosoundings and special tethered balloon soundings for the lowest level ( $z \leq 500$  m).

### 2.2.2.- Oceanic upper layer

Although the general equations are similar, the approach of the problem has been to a slight extent different in the case of the oceanic mixed layer and thermocline. Efforts have been made to solve equations (19) to (23) using similar techniques as in the atmosphere, but much emphasis has been laid on integrated models, capable of simulating the time evolution

4. The buoyancy flux can be obtained from 2 and 3 :

$$\overline{w'b'_0} = \frac{\alpha g}{\rho_0 c_p} [H + E + I' - I'' - I_0 r - \rho_0 c_p (T_p - T_s)] - \beta g (P - \frac{E}{\rho_0 L}) S_0 \quad (39)$$

$$5. \quad \overline{\frac{1}{2} w' (u'^2 + v'^2 + w'^2) + \frac{p' w'}{\rho_0}} \quad (40)$$

This is the flux of the turbulent velocity and pressure fluctuations. Near the surface, it must be equal to the rate of working by the wind, and is usually parameterized as  $-c_1 u^3$  where  $c_1$  is a proportionality factor.

b) Bottom boundary.

Below the mixed layer, the turbulence and turbulent fluxes vanish. If we integrate the equations, this process leads to special boundary conditions detailed below.

#### 2.2.2.1.- Non integrated models

Mixing length hypotheses are also used in the ocean. The main problem is to find a good parameterization for the eddy diffusivities. In Mellor and Durbin's model (1975)

$$- \overline{(u'w')}, \overline{(v'w')} = e^{\frac{1}{2}} \ell S_M \left( \frac{\partial u}{\partial z}, \frac{\partial v}{\partial z} \right)$$

$$- \overline{w'T'} = e^{\frac{1}{2}} \ell S_T \frac{\partial T}{\partial z}$$

where  $S_M(R_i)$  and  $R_T(R_i)$

$$\left[ R_i = \frac{\frac{\partial b}{\partial z}}{\left[ \frac{\partial u}{\partial z} \right]^2 + \left[ \frac{\partial v}{\partial z} \right]^2} \right]$$

take the effect of static stability on the eddy coefficients into account. The  $S(R_i)$ 's have been estimated using higher order closure hypotheses and laboratory experimental results.

A simplified turbulent kinetic energy balance neglecting diffusion and assuming local equilibrium is also used.



$$-\overline{u'w'} \frac{\partial u}{\partial z} - \overline{v'w'} \frac{\partial v}{\partial z} + \overline{b'w'} - \epsilon = 0$$

$$\epsilon = c e^{\frac{3}{2}} \ell^{-1}$$

where  $c$  is a constant and  $\ell$  is defined as

$$\frac{1}{\ell} = \frac{1}{-Kz} + \frac{1}{\ell_-}$$

and

$$\ell_- = -c' \frac{\int_{-}^0 e z dz}{\int_{-}^0 e dz}$$

where  $c'$  is another constant.

These models make no assumption concerning the existence of a mixed layer. They give realistic profiles with mixed layers and thermoclines, but they require much computation work and leave some important physical processes apart.

#### 2.2.2.2.- Integrated models

If we assume that there exists a well mixed layer (temperature, salinity, and to a lesser extent, current), we obtain the so-called slab models, and equations can be integrated over the mixed layer depth  $h$  (from  $-h$  to  $0$ ) :

$$h \frac{du}{dt} = fvh - \overline{u'w'_0} + \overline{u'w'_{-h}} \quad (41)$$

$$h \frac{dv}{dt} = -fuh - \overline{v'w'_0} + \overline{v'w'_{-h}} \quad (42)$$

$$h \frac{dT}{dt} = -\overline{w'T'_0} + \overline{w'T'_{-h}} + \frac{1}{\rho_0 c} I_0 (1-r) (1 - e^{-\gamma h}) \quad (43)$$

$$h \frac{dS}{dt} = -\overline{w'S'_0} + \overline{w'S'_{-h}} \quad (44)$$

$$h \frac{de}{dt} = \text{Prod} + \int_{-h}^0 \overline{b'w'} dz - \left[ \frac{\overline{p'w'}}{\rho_0} + \frac{\overline{w'}}{2} (u'^2 + v'^2 + w'^2) \right]_0 + \left[ \frac{\overline{p'w'}}{\rho_0} + \frac{\overline{w'}}{2} (u'^2 + v'^2 + w'^2) \right]_{-h} - \text{Diss} \quad (45)$$

Here,  $u$ ,  $v$ ,  $T$ ,  $S$  and  $e$  denote the values of the variables in the mixed layer, and geostrophic current has been omitted.

These equations involve the fluxes at the bottom boundary of the mixed layer. Taking into account the fact that discontinuities are possible at the bottom of the mixed layer for temperature, salinity, current and kinetic energy, the bottom boundary fluxes can be expressed as :

$$\overline{u'w'_{-h}} + W_e u = 0 \quad (46)$$

$$\overline{v'w'_{-h}} + W_e v = 0 \quad (47)$$

$$\overline{w'T'_{-h}} + W_e (T - T_b) = 0 \quad (48)$$

$$\overline{w'S'_{-h}} + W_e (S - S_b) = 0 \quad (49)$$

$$\left[ \frac{\overline{p'w'}}{\rho_0} + \frac{\overline{w'}}{2} (u'^2 + v'^2 + w'^2) \right]_{-h} + W_e e - W_e \frac{1}{2} (u^2 + v^2) = 0 \quad (50)$$

where the subscript  $b$  denotes the values in the layers below the mixed layer.

The value  $W_e$  appearing in the equations is the rate of entrainment of the underlying fluid into the mixed layer, and it is equal to the time derivative of the mixed layer depths when this is increasing. However, when the depth of the mixed is decreasing, it is assumed to be completely decoupled from the ocean interior and  $W_e = 0$ . The physical meaning of this assumption is the fact that the ocean mixed layer cannot demix. This can be collected in a formal way using the Heaviside function

$$\theta(x) = \begin{cases} 1 & \text{if } x \geq 0 \\ 0 & \text{if } x \leq 0 \end{cases}$$

$$W_e = \frac{dh}{dt} \theta \left( \frac{dh}{dt} \right) .$$

If we introduce equations (46) to (50) into equations (41) to (45), we get after a little algebra :

$$\frac{d}{dt} (h u) - f v h = \frac{\tau_{0x}}{\rho_0} \quad (51)$$

$$\frac{d}{dt} (h v) + f u h = \frac{\tau_{0y}}{\rho_0} \quad (52)$$

$$h \frac{dT}{dt} = - W_e (T - T_b) - \overline{w'T'_0} + \frac{1}{\rho_0 c} I_0 (1-x) (1 - e^{-\gamma h}) \quad (53)$$

$$h \frac{dS}{dt} = - W_e (S - S_b) - \overline{w'S'_0} \quad (54)$$

$$\begin{aligned} W_e \left\{ \frac{h}{2} [\alpha g (T - T_b) - \beta g (S - S_b)] + e - \frac{1}{2} (u^2 + v^2) \right\} &= \text{Prod}_s + c_1 u_*^3 \\ + \frac{h}{2} \overline{b'w'_0} - \frac{h}{2} \frac{\alpha g}{\rho_0 c} I_0 (1-x) \left[ 1 - \frac{2}{\gamma h} + e^{-\gamma h} \left( 1 + \frac{2}{\gamma h} \right) \right] &- \text{Diss} \end{aligned} \quad (55)$$

Equation (II.27) is used as a balance, i.e.  $h \frac{de}{dt} \approx 0$ . The production of turbulent kinetic energy is zero in the layer since there is no shear ( $u$  assumed constant). Shear can act at the bottom of the layer [third term on the left hand side of (55)], and also in a thin layer close to the surface and driven mainly by wind ( $\text{Prod}_s$ ).  $\text{Prod}_s$  can be parameterized by  $c_2 u_*^3$  where  $c_2$  is a proportionnality factor. Production at the surface and turbulent flux can be taken together and  $u_{**}^3 = c_1 u_*^3 + c_2 u_*^3$  used as a new turbulent velocity scale.

The problem now is to find a good parameterization for the energy dissipation. As the turbulent kinetic energy has three major sources :

- Production plus flux at the surface =  $u_{**}^3 = \text{Prod}_{\text{surf}}$
- Production due to shear at the bottom =  $W_e \frac{1}{2} (u^2 + v^2) = \text{Prod}_{\text{shear}}$
- Production due to buoyancy flux at the surface =  $\frac{h}{2} \overline{b'w'_0}$  (if  $\overline{b'w'_0} > 0$ )  
=  $\text{Prod}_{\text{buoy}}$  ;

the dissipation rate is written as a sum of three parts corresponding to each particular source :

$$\text{Diss} = (1 - \phi_1) \text{Prod}_{\text{shear}} + (1 - \phi_2) \text{Prod}_{\text{surf}} + (1 - \phi_3) \text{Prod}_{\text{buoy}}.$$

Again,  $e$  is assumed to be of the order of  $u_{**}^2$  (or  $u_*^2$ ). This leads to

$$\begin{aligned} w_* \left\{ \frac{h}{2} [\alpha g(T - T_b) - \beta g(S - S_b)] + c u_{**}^2 - \phi_1 \frac{1}{2} (u^2 + v^2) \right\} \\ = \phi_2 u_{**}^2 + \frac{h}{4} [(1 + \phi_3) \overline{b'w'_0} - \frac{1 - \phi_3}{\overline{b'w'_0}}] \\ - \frac{h}{2} \frac{\alpha g}{\rho_0 c} I_0 (1 - r) \left[ 1 - \frac{2}{\gamma h} + e^{-\gamma h} \left( 1 + \frac{2}{\gamma h} \right) \right] \end{aligned}$$

In the first applications,  $\phi_1$ ,  $\phi_2$  and  $\phi_3$  were taken as constant. Recently, Kitaigorodskii developed the model for particular cases of deepening and by comparison with well documented laboratory data, he got expressions of  $\phi_1$  and  $\phi_2$  as a function of the bulk Richardson number

$$Ri_{**} = \frac{h[\alpha g(T - T_b) - \beta g(S - S_b)]}{u_{**}^2}.$$

Such models can describe the time evolution of the mixed layer if they are well calibrated.

Further improvements we would like to develop are the following :

- the development of an integrated model in parallel with a non integrated one. This will shed some light on the general validity of the parameterization of the integrated model.
- the modification of these models to introduce other effects as internal waves, e.g.
- the search for stationary or quasi-stationary solutions for this problem, and their conditions of existence.

### 3.- Climatic problems related to air-sea interactions

#### 3.1.- DEFINITION OF THE PROBLEM AND JUSTIFICATION

The necessity of a better understanding of climate and climatic changes has become evident nowadays. As climatic fluctuations are governed by the climatic system components, in which the oceanic system takes a prominent part, it is understandable that the European Commission for Research in the field of climatology asks the oceanographers to undertake more research dealing with climatic problems.

Among these, some play a leading part because of their serious social and economic consequences : coldest winters for a long time in England (1962-63), USSR, Turkey (1971-72) ; highest summer temperatures and following drought in USSR, Finland and Western Europe ; persistent drought in the major countries of the Third-World : Chile (1960-69), Mexico, Sahel and Cape Verde Islands (1968-73) ; catastrophic floods all over the world (even in the central Australian desert).

The W.M.O. (World Meteorological Organization) understood it well, and its efforts to solve these problems are constant, for example through international research programs as IDOE (International Decade of Ocean Exploitation), GARP (Global Atmosphere Research Program), GATE (GARP Atlantic Tropical Experiment), WAMEX (West African Monsoon Experiment).

The problem of drought in the Sahel related to the upwelling phenomenon in the Gulf of Guinea that we are investigating is well at its place in this context.

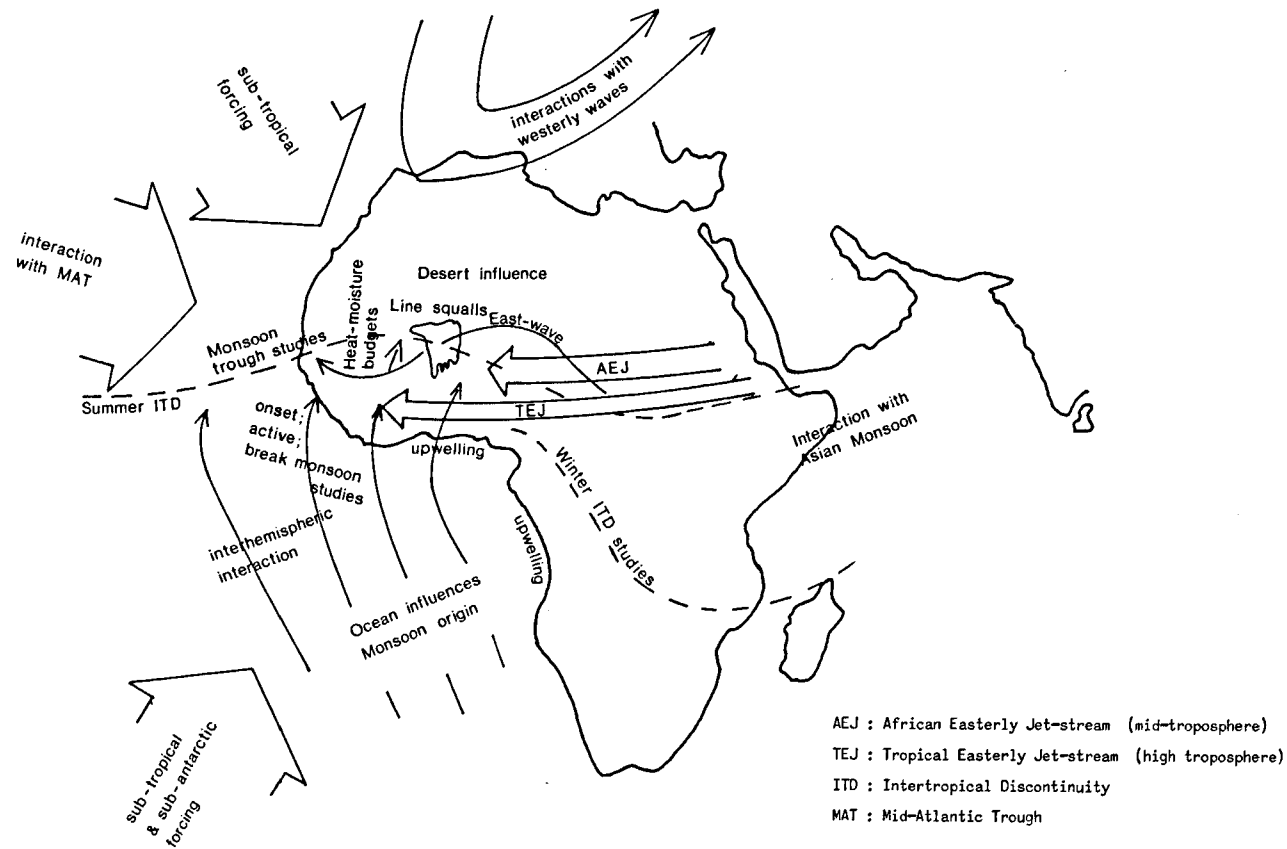
Many arguments plead in favour of this study, which are of :

#### 1. Geographical nature :

The tropical situation of this zone first, and secondly, the proximity of the equatorial region allow theoretical studies required by meteorologists about the energetic equator fluctuations and the equatorial atmospheric and oceanic circulations (cfr. GARP), especially the ascending branch of the Hadley cell;

#### 2. Physical nature :

- On the one hand, the existence of monsoon winds due to ocean-continent thermal gradients because of the permanent conflict between air masses under the direct influence of Açores, St. Helene and Libye anticyclones, and Saharian and equatorial troughs,



After WAMEX (1976).

fig. 6.

- and on the other hand, the occurrence of coastal and oceanic upwelling in the Gulf of Guinea just under the fetch zone of monsoons, are the best way to an adequate approach of any study of the ocean-atmosphere-continent hydrological cycle, and thus, of the pluviosity in the Sahel.

Moreover, interactions with extratropical zones (figure 6) support the interpretation of the extratropical role which is to be played by this region : eventual correlations for climatic anomalies between the Mediterranean Basin and the Sahel zone ; European and American atmospheres pollution by saharian sands, and who knows, tomorrow, perhaps with dust, CO<sub>2</sub> and ashes due to the burning of the bush used by the sahelian traditional agriculture ? In the same way, the incursions in the Sahel of the high latitudes circulation must be noticed, as well as the reject of the subtropical anticyclone belt towards mid-latitudes.

The basic idea of this study is the following : as precipitations are function of the water-vapour content of the air masses over the continent, the variation in the intensity of oceanic evaporation related to any loss all along the ocean-atmosphere-continent hydrological cycle could explain the abnormal deficit of pluviosity in the Sahel area, and thus, the increasing risk of drought and aridification.

### 3.2.- THE UPWELLING IN THE GULF OF GUINEA

In order to understand the generation and the development of the upwelling in the Gulf of Guinea, we try to discern the eventual role of local effects from that of external effects :

- are the fundamental causes of purely oceanic origin (trade wind regime variation exciting a Kelvin wave propagating eastward along the equator),
- or are they of local character with south-west trade winds (monsoons), topographic effects and irregular coastline (existence of capes and bights) playing the fundamental part ?

The mathematical model used is the following :

$$\frac{\partial u}{\partial t} + u \frac{\partial u}{\partial x} + v \frac{\partial u}{\partial y} = \beta y v - g' \frac{\partial h}{\partial x} + \frac{\tau_x}{\rho_H} + A \left( \frac{\partial^2 u}{\partial x^2} + \frac{\partial^2 u}{\partial y^2} \right)$$

$$\frac{\partial v}{\partial t} + u \frac{\partial v}{\partial x} + v \frac{\partial v}{\partial y} = -\beta y u - g' \frac{\partial h}{\partial y} + \frac{\tau_y}{\rho_H} + A \left( \frac{\partial^2 v}{\partial x^2} + \frac{\partial^2 v}{\partial y^2} \right)$$

$$\frac{\partial h}{\partial t} + \frac{\partial}{\partial x} [(H+h)u] + \frac{\partial}{\partial y} [(H+h)v] = 0$$

where  $u$ ,  $v$  and  $h$  describe perturbations of horizontal circulation and upper layer thickness (fluctuations of pycnocline);  $\beta$  is the Rossby parameter,  $\tau_{x,y}$  the components of the surface wind stress in the east and north directions, respectively.  $g'$  is the reduced gravity

$$g' = g \frac{\rho_2 - \rho_1}{\rho_2}.$$

$\rho$  ( $= \rho_1$ ) is the density of the upper layer,  $H$  is its mean thickness and  $A$  the horizontal eddy viscosity coefficient.

Introducing non dimensional parameters, we get

$$\frac{\partial u}{\partial t} + a_1 u \frac{\partial u}{\partial x} + v \frac{\partial v}{\partial y} = yv - a_1 \frac{\partial h}{\partial x} + a_2 \frac{\tau}{\rho} + a_3 \frac{\partial^2 u}{\partial x^2} + a_4 \frac{\partial^2 u}{\partial y^2}$$

$$\frac{\partial v}{\partial t} + a_1 u \frac{\partial v}{\partial x} + v \frac{\partial v}{\partial y} = -yu - \frac{\partial h}{\partial y} + a_2 \frac{\tau}{\rho} + a_3 \frac{\partial^2 v}{\partial x^2} + a_4 \frac{\partial^2 v}{\partial y^2}$$

$$\frac{\partial h}{\partial t} + a_1 u \frac{\partial h}{\partial x} + v \frac{\partial h}{\partial y} + a_1 (H+h) \frac{\partial u}{\partial x} + (H+h) \frac{\partial v}{\partial y} + a_1 u \frac{\partial H}{\partial x} + v \frac{\partial H}{\partial y} = 0$$

where

$$a_1 = \frac{L_y}{L_x},$$

$$a_2 = \beta^{-\frac{1}{2}} g^{-\frac{3}{4}} (H+h)^{-\frac{7}{4}},$$

$$a_3 = A \frac{W^2}{L^2} \beta^{\frac{1}{2}} g' (H+h)^{-\frac{3}{4}},$$

$$a_4 = A \beta^{\frac{1}{2}} [g' (H+h)]^{-\frac{3}{4}};$$

$$W = \frac{\sqrt{g' (H+h)}}{\beta L_x};$$

$L_x$  and  $L_y$  are the zonal and meridional length scales respectively.



The dimensional analysis shows that, for a constant  $H$  (50 m), the wind forcing term  $a_2$  plays the fundamental role :

$$\frac{a_1}{a_2} \sim 10^{-3} \quad , \quad \frac{a_3}{a_2} \sim 10^{-6} \quad , \quad \frac{a_4}{a_2} \sim 10^{-7} .$$

With such a model, we can predict, as soon as meteorological forcings are known, the intensity and the duration of the upwelling, and further, if a thermal equation is associated, the sea surface temperature (SST), that could allow the quantification and the analysis of energetic exchanges (latent and sensible heat) in the Gulf of Guinea, and consequently, an approach of the hydrological cycle and its influence on the pluviosity in the Sahel.

Preliminary results confirm the general theoretical characteristics already described by O'Brien et al. (1978) :

- eastward propagating perturbation along the Equator, generating an upwelling of 12 m on the tenth day, with an east-west perturbation velocity  $u = - 0.41$  m/s ;
- full upwelling in the entire Gulf of Guinea on about day 50, with the maximum value centered at the Equator.

### 3.3.- DATA ANALYSIS AND INTERPRETATION

The theoretical study is completed by the analysis of climatic data (precipitations and run-off in the Sahel, SST in the Gulf of Guinea).

Up to now, the only available data are precipitations for 20 stations and a 69 years period (figure 7). The curve on figure 8 is somewhat like that of Bunting et al. (1976) and shows periods of extreme drought (1913, 1940, 1970). Bunting et al. used only five stations. Our curve uses more stations and is thus better for the zonally averaged means, as recommended by the WMO, because of the high spatial variability of convective rainfall in the Sahel region. The great difference is the peak for the year 1966. However, this value is doubtful and must be related to the surprising maximum monthly value of April 1966 (208 mm, i.e. 26 % of the total annual rainfall in 1966).



fig. 7.

Rainfall stations in West Africa used in the zonal mean

So, the only values for the 4 months period - june to september - are considered further. The choice of this period can be justified as follows :

1. 91 % of the rainfall occur during these 4 months (Bunting et al., 1976);
2. the maximum pluviosity cannot occur in april, but in july and (or) august, when the ITF (Intertropical Front) reaches its northeast position, whereas, even in may, the ITF lies in Conakry ( $9^{\circ}30'N$ ), far south from the Sahel zone, whose lowest latitude station is Maidugury ( $10^{\circ}47'N$ );
3. rainy monsoon winds blow over the upwelling zone in the Gulf of Guinea during this chosen period.

The resulting curve (figure 9) is more similar to that of Bunting et al (1976) and depicts the general tendency of a decreasing pluviosity during the last thirty years.

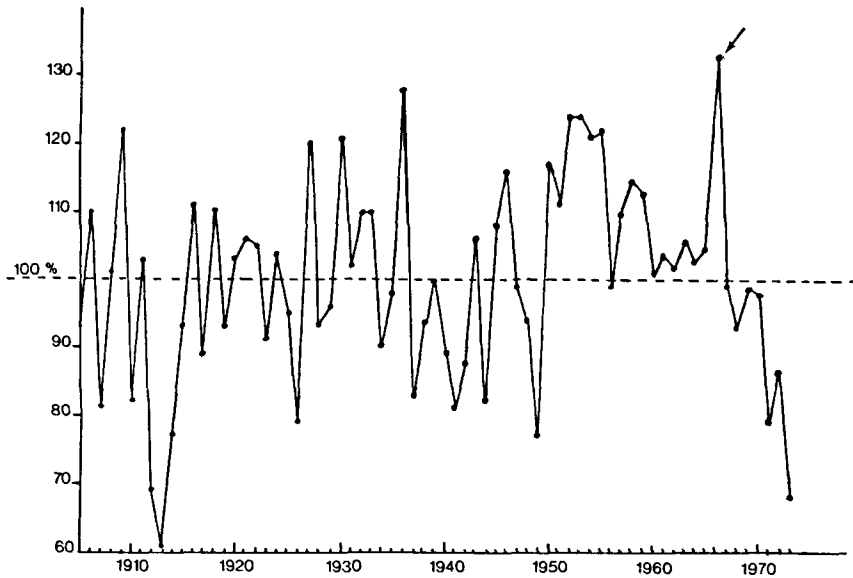


fig. 8.

Mean annual rainfall for the 20 sahelian stations  
expressed as a percentage of the normal 1905-1973.

Fourier analysis has been performed for the annual means, and the spectrum shows peaks at several frequencies (figure 10 and table 3).

Table 3

Period (years per cycle) observed by spectral analysis of zonal mean rainfall  
in the Sahel (Bah, Bunting et al.) and temperatures in Central England (Mason).  
Values of % of total variance are underlined.

MASON (1976)	23	14.5	11.5	7.6	5.2	3.5	3.1	2.8	2.5	2.2	2.1	
	<u>8</u>		<u>&lt; 4</u>								<u>10</u>	
BUNTING et al. (1976)	40	20	10	6.7	5.0	4.0	3.3	2.9	2.5	2.2	2.1	
	<u>7.2</u>	<u>10.5</u>	<u>12.4</u>	<u>10.3</u>	<u>5.7</u>	<u>5.5</u>	<u>8.9</u>	<u>9.9</u>	<u>12.7</u>	<u>12.7</u>	<u>9.7</u>	
BAH (1979)	34.5	11.5	6.9	4.9	4.3	3.9	3.5	3.1	2.8	2.5	2.4	2.2
	<u>13.2</u>	<u>11.7</u>	<u>3.2</u>			<u>5.1</u>		<u>9.8</u>	<u>5.1</u>		<u>7.5</u>	

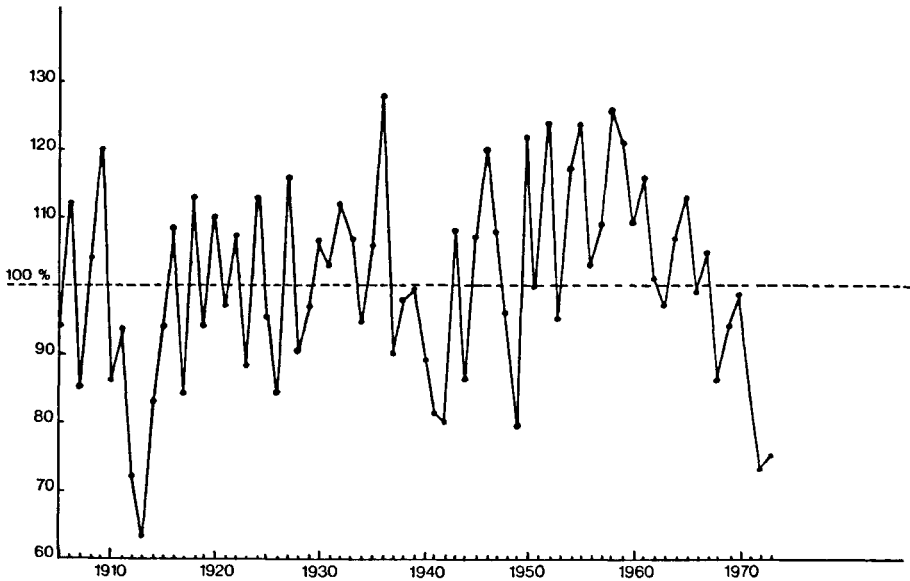


fig. 9.

Mean rainfall for the 4-months period (June, July, August, September) expressed as a percentage of the corresponding normal 1905-1973.

The 11.5 years periodicity may be identified with the semi-period of the "double sunspot cycle" or Hale cycle.

The 7.1. years peak suggests the periodicity of 8 years observed over Lake Victoria, which is very regular and which may be associated with solar activity.

Lower periodicities could perhaps be related to the cycles of suspended particles,  $\text{CO}_2$ , ice blocks, sea level pressure, coastal upwelling easterly perturbations, Arctic temperature anomaly, or other climatic features.

These preliminary results should be confirmed by further studies. Nevertheless, it is surprising to notice that Bunting et al (1976), as well as Mason (1976) obtain similar periodicities, especially at high frequencies, with temperature data series in Central England (1668-1975) (table 3).

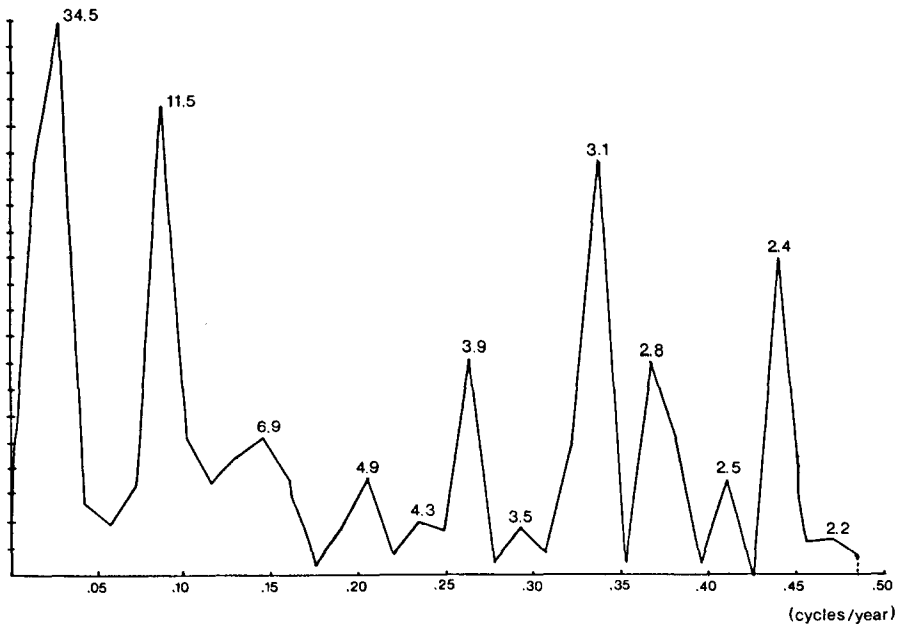


fig. 10.

Power spectrum of the zonal mean rainfall record

Does this result imply that mid-latitudes and subtropical latitudes are under the influence of the same high frequency phenomena at short climatic scales ? Or could there be some interaction, may be linear, between meteorological and climatic phenomena of these different latitudes ?

There is another hypothesis : the persistence of polar air masses in the subtropical atmosphere in the form of cold air drops, and thus, the influence of polar front fluctuations on the climatology of the Sahel. If so, there is a need for further studies of the possible correlations between climatic phenomena of subtropical zones and corresponding phenomena not only in the Mediterranean Basin (Helbig, 1976), but also in higher latitude zones.

For fitting purpose, Bunting et al (1976) gave the curve :

$$R = - 12.7 + 12.9 \sin \frac{2\pi(t + 12)}{180} ,$$

but they underlined that it provides no basis for forecasting. The curve we propose is the following, and it contains 84 % of the total variance :

$$\begin{aligned}
 R = & - 6.62 \cos \left( \frac{2}{69} \pi t - 63^\circ 56 \right) - 7.63 \cos \left( \frac{4}{69} \pi t - 33^\circ 62 \right) \\
 & - 7.02 \cos \left( \frac{4}{23} \pi t - 49^\circ 33 \right) + 4.72 \cos \left( \frac{12}{23} \pi t - 58^\circ 35 \right) \\
 & - 6.64 \cos \left( \frac{46}{69} \pi t - 57^\circ 4 \right) - 4.71 \cos \left( \frac{50}{69} \pi t - 6^\circ \right) \\
 & - 5.07 \cos \left( \frac{20}{23} \pi t + 2^\circ 97 \right) + 3.84 \cos \left( \frac{20}{69} \pi t + 47^\circ 6 \right) \\
 & - 3.71 \cos \left( \frac{14}{69} \pi t + 58^\circ 77 \right) - 3.73 \cos \left( \frac{44}{69} \pi t + 41^\circ 67 \right) \\
 & - 3.77 \cos \left( \frac{52}{69} \pi t - 54^\circ 56 \right)
 \end{aligned}$$

where  $R$  is the % deviation from the 1905-1973 mean and  $t$  is the time in years.

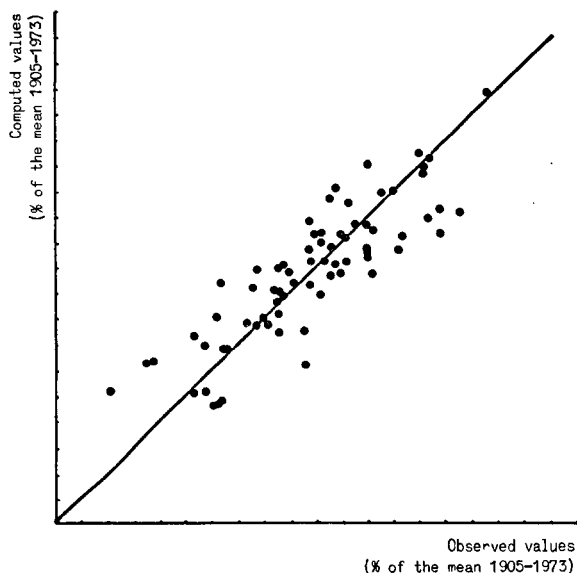


fig. 11.

Observed values versus computed values for  $R$

Computed values and observed ones are plotted on figure 11.

We intend to perform the same analysis on SST data series, as soon as they become available, in order to get significant periodicities of anomalies eventually related to continental rainfall variations.

An efficient collaboration could be established with IRM (Institut Royal Météorologique de Belgique) and LMD (Laboratoire de Météorologie Dynamique, Palaiseau, France).

## References

- BUNTING, A.H., DENNETT, M.D., ELSTON, J. and MILFORD, J.R., 1976. Rainfall trends in the West African Sahel, *Quart. J. R. Met. Soc.*, 102 (431), 59-64.
- BUSINGER, J., 1973. Turbulent transfer in the atmospheric surface layer, *Workshop on Micrometeorology*, Am. Met. Soc., pp. 67-100.
- CHAMPAGNE, F.H., FRIEHE, C.A., LA RUE, J.C. and WYNGAARD, J.C., 1977. Flux measurements, flux estimation techniques, and fine scale turbulence measurements in the unstable surface layer over land, *J. Atmos. Sci.*, 34, 515-530.
- CLEMENT, F., 1979. *Analyse des données de la bouée IRM à Calvi*, Mémoire de licence en sciences physiques, U.C.L.
- COANTIC, M., 1978. *An introduction to turbulence in geophysics and air-sea interactions*, Agardagraph n° 232.
- FEDOROV, K.N., 1978. *The thermohaline finestructure of the ocean*, Pergamon Marine Series, Pergamon Press, 2, 1-170.
- FRIEHE, C.A. and GIBSON, C.H., 1978. Estimates of surface fluxes over the ocean, in *Turbulent fluxes through sea surface, wave dynamics and prediction*, A. Favre and K. Hasselman (Editors), NATO Conf. Series, pp. 67-80.
- HELBIG, M., 1976. *Korrelations - und Spectrum Analyse von Niederschlägen - und Abflussreihen aus Afrika und Reduktion der Niederschlagsdaten durch Gebietsmittelung*, Diplomarbeit, Meteorologisches Institut der Universität Bonn.
- KITAigorodskii, S.A., 1973. *The physics of air-sea interaction*, Israël Prog. Sci. Trans.
- KITAigorodskii, S.A., 1978. Review of the theories of wind-mixed layer deepening, in *Marine Forecasting*, J.C.J. Nihoul (Editor), Elsevier, Oceanography Series, Amsterdam.
- KRAUSS, E.B., 1972. *Atmosphere-ocean interactions*, Oxford Monographs on Meteorology, Oxford University Press.
- KRAUSS, E.B., 1977. *Modelling and prediction of the upper layers of the ocean*, Pergamon Marine Series, Pergamon Press, 1, 1-325.

- MASON, B.J., 1976. Towards the understanding and prediction of climatic variations, *Quart. J. R. Met. Soc.*, 102 (433), 473-498.
- MELLOR, G.L. and DURBIN, P.A., 1975. The structure and dynamics of the ocean surface mixed layer, *J. Phys. Oceanogr.*, 5, 718-728.
- O'BRIEN, J.J., ADAMEC, D. and MOORE, D.W., 1978. *A simple model of upwelling in the Gulf of Guinea*, Contribution of the Geophysical Fluid Dynamics Institute, Florida State University.
- SCHAYES, G., 1979. *Profils K utilisés dans les modèles simples de la couche limite atmosphérique*, Scientific Report 1979/2, U.C.L.
- YU, T.W., 1977. A comparative study on parameterization of vertical turbulent exchange processes, *Mon. Weather Rev.*, 105, 57-66.